Neoplasia • Vol. 7, No. 5, May 2005, pp. 466–474 466

www.neoplasia.com

Acute Tumor Response to ZD6126 Assessed by Intrinsic Susceptibility Magnetic Resonance Imaging[1]

Simon P. Robinson, Tammy L. Kalber*, Franklyn A. Howe*, Dominick J. O. McIntyre*, John R. Griffiths*, David C. Blakey†, Lynsey Whittaker†, Anderson J. Ryan† and John C. Waterton‡*

*Department of Basic Medical Sciences, St. George's Hospital Medical School, London SW17 ORE, UK; †Department of Cancer and Infection Research, AstraZeneca, Alderley Park, Macclesfield, Cheshire SK10 4TG, UK; ‡Department of Imaging, Global Sciences and Information, AstraZeneca, Alderley Park, Macclesfield, Cheshire SK10 4TG, UK

Abstract

The effective magnetic resonance imaging (MRI) transverse relaxation rate R_2* was investigated as an early acute marker of the response of rat GH3 prolactinomas to the vascular-targeting agent, ZD6126. Multigradient echo (MGRE) MRI was used to quantify R_2*, which is sensitive to tissue deoxyhemoglobin levels. Tumor R_2* was measured prior to, and either immediately for up to 35 minutes, or 24 hours following administration of 50 mg/kg ZD6126. Following MRI, tumor perfusion was assessed by Hoechst 33342 uptake. Tumor R_2* significantly increased to 116 ± 4% of baseline 35 minutes after challenge, consistent with an ischemic insult induced by vascular collapse. A strong positive correlation between baseline R_2* and the subsequent increase in R_2* measured 35 minutes after treatment was obtained, suggesting that the baseline R_2* is prognostic for the subsequent tumor response to ZD6126. In contrast, a significant decrease in tumor R_2* was found 24 hours after administration of ZD6126. Both the 35-minute and 24-hour R_2* responses to ZD6126 were associated with a decrease in Hoechst 33342 uptake. Interpretation of the R_2* response is complex, yet changes in tumor R_2* may provide a convenient and early MRI biomarker for detecting the antitumor activity of vascular-targeting agents.

Neoplasia (2005) **7,** 466–474

Keywords: ZD6126, vascular-targeting agents, MRI, tumor perfusion, response biomarker.

Introduction

It is now well-established that the development, growth, and survival of solid tumors are highly dependent on a functional vascular network [1]. Established blood vessels, which consist of endothelial cells, support cells, and a basement membrane, provide tumor cells with oxygen and nutrients, and enable the removal of toxic waste products of cellular metabolism. Physiological angiogenesis is a tightly regulated process that occurs only in a limited number of situations such as wound healing or during the menstrual cycle. In contrast, in several pathologic situations, including cancer, angiogenesis is dysregulated [2]. As a result, tumor vasculature has a very different morphology compared with normal tissues. For example, in a normal adult, most of the vascular endothelium is quiescent, with only 0.01% of endothelial cells undergoing division, whereas in tumors, the expression of proangiogenic growth factors can result in an endothelial cell proliferation rate 35-fold higher than that of normal tissues [3,4]. Differences between normal and tumor endothelium are now being exploited with novel therapies to selectively target the proliferating tumor endothelium while leaving the normal blood vessels relatively unaffected [5]. This strategy has several advantages. In particular, the dependence of tumor cells on functional blood vessels means that damage to relatively few endothelial cells could result in the death of many tumor cells [2,6–8].

ZD6126 (*N*-acetylcolchinol-*O*-phosphate) is a vascular-targeting agent shown to have significant antitumor effects, both against a wide range of rodent and human tumor model systems [9–17] and against human tumor vasculature in the clinic [15]. ZD6126 is rapidly converted by serum phosphatases to *N*-acetylcolchinol (NAC), and studies *in vitro* have shown that NAC disrupts the tubulin cytoskeleton and induces rapid changes in the endothelial cell morphology of proliferating, but not confluent, endothelial cells [18]. *In vivo*, disruption of the tumor endothelium has been shown within an hour of ZD6126 administration [11], with these early changes followed by thrombosis and vessel occlusion resulting in massive central tumor necrosis 24 hours after treatment. A common

Address all correspondence to: Simon Robinson, Department of Basic Medical Sciences, St. George's Hospital Medical School, Cranmer Terrace, London SW17 ORE, UK. E-mail: s.robinson@sghms.ac.uk

[1]This work was supported by The Royal Society, AstraZeneca, BBSRC, and Cancer Research UK (grant C12/A1209). S.P.R. is the recipient of a Royal Society University Research Fellowship.

Received 23 September 2004; Revised 11 November 2004; Accepted 12 November 2004.

DOI 10.1593/neo.04622

histologic observation is the existence of a viable rim of tumor cells that survives treatment with ZD6126. Vascular-targeting agents alone typically result in tumor growth delay, but not regression—presumably a consequence of continued growth from this surviving viable rim [10–12].

Methods for the assessment of tumor vasculature are continually being sought to provide quantitative sensitive indices of tumor pathophysiology and response that can be translated to the clinic [19,20]. As many vascular-targeting agents are not expected to induce rapid tumor regressions as single-agent therapies, their clinical development will benefit greatly from the use of biomarkers. In particular, magnetic resonance imaging (MRI) provides a number of potential imaging biomarkers associated with tumor blood vasculature and its response to therapy, which require evaluation before they can be deployed in clinical trials. Dynamic contrast-enhanced (DCE) MRI has been used to demonstrate the dose-dependent activity of ZD6126 in two rodent tumor models, rat GH3 prolactinomas [14] and murine colon 38 carcinomas [15]. In particular, the effect of 50 mg/kg ZD6126 on rat GH3 prolactinomas was profound 24 hours after administration. However, DCE MRI is unsuited to hyperacute measurements because several hours must elapse between measurements to permit contrast agent elimination.

We are currently further investigating the use of intrinsic susceptibility MRI, which utilizes endogenous deoxyhemoglobin as the primary source of image contrast, to assess tumor response to ZD6126. Deoxyhemoglobin is paramagnetic and its presence creates magnetic susceptibility perturbations around blood vessels, thus increasing the effective transverse magnetic resonance relaxation rate R_2* of the surrounding tissue in proportion to the tissue deoxyhemoglobin concentration. In the absence of other changes, R_2* depends on tissue deoxyhemoglobin levels and hence may provide an acute index of changes in tissue oxygenation. We originally hypothesized that following treatment with ZD6126, hemoglobin within erythrocytes would deoxygenate, resulting in an increase in tumor R_2*. Intriguingly, in a pilot study designed to establish efficacy of ZD6126 on rat GH3 prolactinomas, tumor R_2* was found to *decrease* 24 hours after treatment, and this correlated with massive hemorrhagic necrosis [14]. The aims of the present study were to investigate the use of tumor R_2* as an early acute marker of tumor response to ZD6126 and provide appropriate histologic validation of any MRI findings.

Materials and methods

Animals, Tumors, and Study Protocol

All experiments were performed in accordance with the local ethical review panel, the UKCCCR guidelines [21], and the UK Home Office Animals Scientific Procedures Act 1986. Rat GH3 prolactinomas were grown in the flanks of 27 female Wistar Furth rats [22]. Anesthesia was induced with a 4 ml/kg intraperitoneal injection of fentanyl citrate (0.315 mg/ml) plus fluanisone (10 mg/ml) (“Hypnorm”; Janssen Pharmaceutical, Ltd.), midazolam (5 mg/ml) (“Hypnovel”; Roche), and water (1:1:2). Tumor volume was measured using calipers, assuming an ellipsoidal shape. The mean tumor volume at the time of randomization to treatment groups was 2.43 ± 0.2 cm^3.

Two MRI study protocols were performed. The first was designed to monitor tumor R_2* immediately following administration of ZD6126, whereas the second was designed to measure tumor R_2* and R_2 prior to and 24 hours following treatment with ZD6126.

Intrinsic Susceptibility Contrast MRI—Study 1

MRI was performed on a Varian Unity Inova system interfaced to a 4.7-T horizontal magnet, using a three-turn, 25-mm–diameter imaging coil. A lateral tail vein was cannulated with a 27-G butterfly needle for administration of either ZD6126 or saline. The rats were positioned so that the tumor hung vertically into the imaging coil and covered with a warm water blanket to maintain the core temperature at 37°C. Field homogeneity was optimized by shimming on the water signal for each tumor to a linewidth of ca. 50 Hz.

Multigradient echo (MGRE) images were acquired using a train of eight echoes spaced 5 milliseconds apart, an initial echo time of 5 milliseconds, with a flip angle $\alpha = 45°$ and a repetition time of 80 milliseconds. Images were acquired from five contiguous 1-mm–thick transverse slices through each tumor, using four averages of 256 phase encode steps over a 4 × 4 cm field of view (FOV), giving a temporal resolution of 7 minutes. Two baseline MRI data sets were acquired to enable an assessment of the repeatability of the R_2* measurement, followed by a further five data sets (at 7, 14, 21, 28, and 35 minutes) after administration of either saline, 30 or 50 mg/kg ZD6126, i.v.

Immediately after the final MRI acquisition, the rats were rapidly removed from the magnet bore and injected with 15 mg/kg of the perfusion marker Hoechst 33342 through the tail vein. Hoechst 33342 is a dye that stains the nuclei of endothelial cells, lining blood vessels that are perfused at the time of injection, and thus affords a measure of functional tumor vasculature. One minute later, the rats were sacrificed by cervical dislocation and the tumors rapidly excised and frozen over liquid nitrogen.

Intrinsic Susceptibility Contrast MRI—Study 2

In this study, MGRE MRI was performed on GH3 prolactinomas prior to treatment as described above, except that images were acquired from a single 1-mm–thick transverse slice through the center of each tumor, using eight averages of 256 phase encode steps over a 4 × 4 cm FOV. In addition, spin echo images with TE = 11, 20, 30, and 40 milliseconds, and TR = 300 milliseconds were acquired from the same central slice and FOV. The total imaging time was 14 minutes. The rats were then treated intravenously with either saline or 50 mg/kg ZD6126 and the tumors subsequently imaged again 24 hours later, with the tumor being positioned carefully within the coil so as to afford a degree of registration of the MR images with those acquired prior to treatment. Following MRI, the rats were administered 15 mg/kg Hoechst 33342 and the tumors excised as above.

MRI Data Analysis

Tumor R_2* and R_2 maps for each slice were calculated from the image data sets by fitting a single exponential to the signal intensity echo time curve pixel-by-pixel [23,24]. The mean R_2* and R_2 for each slice from each individual tumor were determined from a region of interest (ROI) encompassing the whole tumor but excluding the surrounding skin/muscle. In addition, for study 2, maps of R_2' (= R_2* − R_2) were synthesized and the mean R_2' determined. Frequency histograms for each slice were also derived from the ROI to assess the distribution of R_2* values.

Fluorescence Microscopy

Contiguous frozen sections through each tumor (10 μm) were subsequently cut on a cryotome in approximately the same plane as for the MRI, and stored at −80°C until processed. Sections were fixed in ice-cold acetone for 10 minutes and then mounted in phosphate-buffered saline. Hoechst 33342 fluorescence signals from whole tumor sections were then recorded at 365 nm using a motorized scanning stage (Prior Scientific Instruments Ltd., Cambridge, UK) attached to a BX51 microscope (Olympus Optical Co. Ltd, London, UK), driven by analysis (Soft Imaging System, Munster, Germany). Digital images from all the tumors were acquired using the same exposure time and composite images were then synthesized [25]. Fluorescent particles were detected above a constant threshold for all the composite images and the area of the tumor section with Hoechst 33342 fluorescence determined and expressed as a percentage of the whole tumor section (mean Hoechst

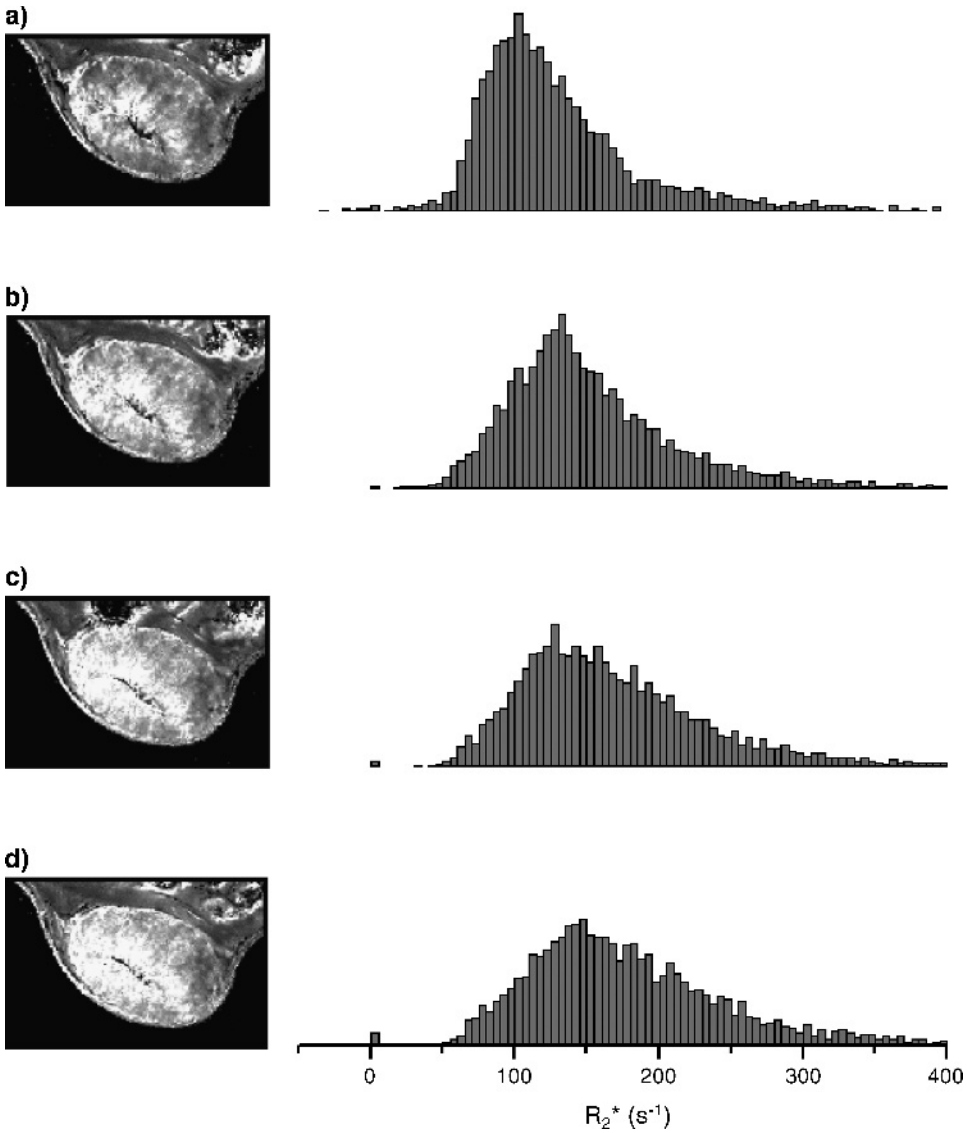

Figure 1. *Tumor R_2* maps and associated frequency histograms obtained from one transverse slice through a rat GH3 prolactinoma (a) prior to, (b) 7 minutes, (c) 21 minutes, and (d) 35 minutes following administration of ZD6126, 50 mg/kg, i.v. The frequency histograms were acquired from an ROI that encompassed the whole tumor but excluded the surrounding skin/muscle. Note the skewing of the distribution of R_2* pixel values toward faster values following administration of ZD6126.*

perfused area, or mHPA). As the images were acquired and analyzed under identical conditions, any differences in mHPA would result from differences in tumor perfusion. Thus these data could be used to validate any changes in intrinsic R_2* contrast induced by ZD6126.

Statistical Analysis

Results are presented in the form mean ± SEM. Unless otherwise stated, significance testing employed the two-tailed *t*-test, assuming unequal variances with a 5% level of significance. Repeatability of the R_2* measurement was assessed using a Bland-Altman plot for differences and confidence intervals, and also by derivation of the intratumoral coefficient of variation [26].

Results

Serial R_2* maps and associated frequency histograms from one GH3 prolactinoma from study 1, treated with 50 mg/kg ZD6126, are shown in Figure 1. For all the tumors studied, the baseline R_2* maps were typically heterogeneous and exhibited a symmetrical distribution of R_2* values. The intratumoral coefficient of variance (rms CoV) for the baseline R_2* measurements within each tumor was 1.7%. Using all the successive baseline R_2* measurements in study 1 before treatment, the repeatability of the R_2* measurement was determined. From the Bland-Altman analysis, the 95% confidence interval between the two pretreatment R_2* measurements was [-9.5 sec^{-1}, 8 sec^{-1}]. This confidence interval contains 0 (i.e., we would fail to reject the null hypothesis that $d = 0$, where d is the difference between the two pretreatment R_2* measurements) and is extremely small compared to the range of R_2* values (83–135 second^{-1}). Application of a paired two-sample *t*-test showed that there was no significant difference between the means of the two baseline R_2* measurements ($P = .52$). Taken together, these findings clearly show an excellent repeatability of the R_2* measurement.

Administration of saline induced no significant change in the R_2* maps and distribution (data not shown), whereas administration of ZD6126 induced a marked increase in R_2* over the first 35 minutes of challenge. Localized increases in R_2* could be discerned qualitatively as early as 7 minutes after administration of ZD6126, with statistically significant increases found 14 minutes post 50 mg/kg ZD6126 ($P < .02$). Visual inspection of the R_2* maps showed that tumor regions exhibiting a relatively fast (intense) basal R_2* showed the greatest increase in R_2* over 35 minutes in response to ZD6126 (Figure 1). The time course of R_2* response for all the tumors in study 1 is shown in Figure 2, which shows that whereas all six saline-treated tumors showed little change in R_2*, 9 of 10 tumors treated with ZD6126 showed an increase in R_2*. To identify any trends within a treatment group, a Jonckheere-Terpstra test was applied to the data. This is a nonparametric test for ordered differences in R_2* among classes (e.g., dose, time), which tests the null hypothesis that the distribution of R_2* does not differ among the classes and thus essentially tests for a monotonic response. No significant trend in response (corrected for baseline values) was observed for the saline-treated group ($P = .28$), whereas for both the 30- and 50-mg/kg treatment groups, a significant monotonic response was observed up to 35 minutes with P values of $P = .0023$ and $P = .0051$, respectively.

Composite fluorescence images of Hoechst 33342 tumor uptake are shown in Figure 3, in which a decrease in tumor perfusion with ZD6126 treatment can be seen. A summary of the data acquired from study 1 is shown in Table 1.

The R_2* maps and frequency histograms shown in Figure 4 were acquired from one GH3 prolactinoma prior to and 24 hours following treatment with 50 mg/kg ZD6126, as part of study 2. Control tumors maintained a relatively

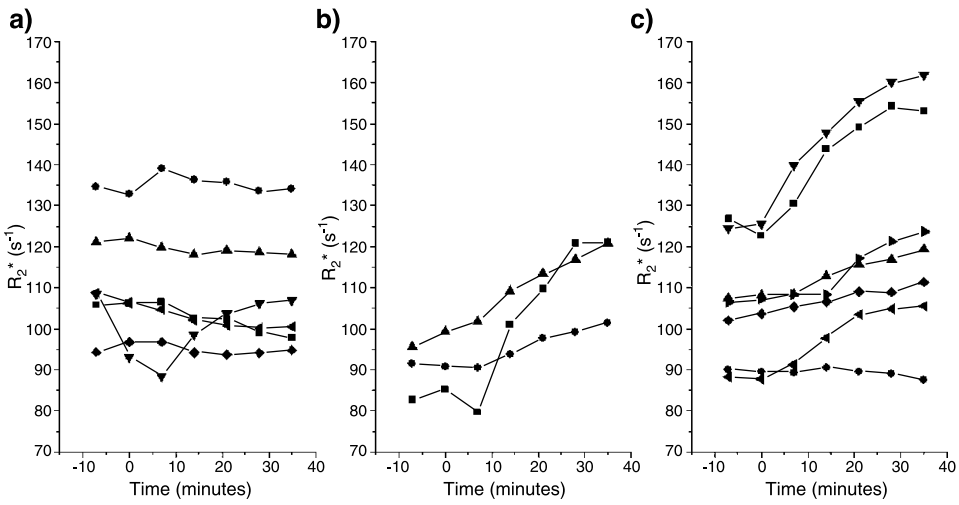

Figure 2. *Profile plots of R_2* (mean R_2* of all five transverse slices) for each individual rat in study 1. Two baseline MGRE MRI data sets to quantify R_2* were acquired prior to intravenous administration of (a) saline (n = 6), (b) 30 mg/kg ZD6126 (n = 3), or (c) 50 mg/kg ZD6126 (n = 7), after which a further five MGRE MRI data sets were acquired. A statistically significant increase in R_2* was found 14 minutes after administration of 50 mg/kg ZD6126 (paired two-sample t-test, P < .02).*

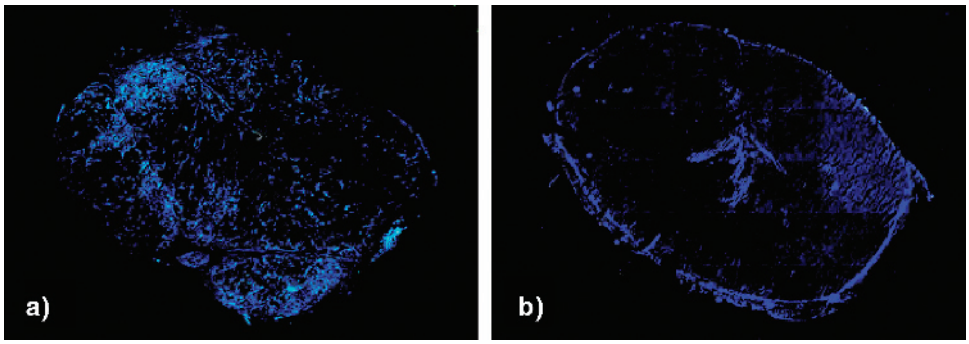

Figure 3. *Composite fluorescence images of Hoechst 33342 uptake into rat GH3 prolactinomas ca. 35 minutes after administration of either (a) saline or (b) 50 mg/kg ZD6126. The composite image shown in (b) is taken from the same tumor shown in Figure 1.*

constant and heterogeneous distribution of R_2* values 24 hours after administration of saline (data not shown). In contrast, treatment with ZD6126 resulted in both a decrease and a more homogeneous distribution of R_2* values over the whole tumor (Figure 4). The individual R_2* values pre- and 24 hours posttreatment for all the tumors in study 2 are shown in Figure 5. All five tumors treated with saline showed a small, nonsignificant R_2* increase 24 hours after challenge, whereas all six tumors treated with ZD6126 showed a striking reduction in R_2*. A similar response was also found for both tumor R_2 and R_2'. As in study 1, composite fluorescence images of Hoechst 33342 tumor uptake revealed a dramatic reduction in the perfusion of ZD6126-treated tumors (Figure 6). The data from study 2 are summarized in Table 2.

The data shown in Figure 2*c* suggest that tumors exhibiting a relatively fast basal R_2* subsequently showed the greatest increase in R_2* 35 minutes after treatment with 50 mg/kg ZD6126. By simply plotting the average baseline R_2* against the change in R_2* at 35 minutes, a correlation would be expected even when there may be no relationship [26]. To overcome this and to test whether the baseline tumor R_2* was predictive for the subsequent magnitude of response to ZD6126, the average of the final and mean baseline R_2* was plotted against the change in R_2* measured 35 minutes after challenge for each tumor (Figure 7). A significant and strong positive correlation was obtained ($r = 0.899$, $P < .01$), which was greater than the correlation of 0.7 we would expect to see by chance [26]. No such correlation was obtained for the tumors imaged 24 hours after treatment with ZD6126 ($r = -0.331$, $P > 0.1$).

Discussion

Noninvasive imaging techniques are continually being developed for the assessment of tumor vascular function and its therapeutic response. As the oxygenation of hemoglobin is proportional to arterial blood p_aO_2 and therefore in equilibrium with tissue pO_2, quantitation of the relaxation rate R_2* by MGRE MRI provides a sensitive index that, under some circumstances, may relate to tissue oxygenation. Furthermore, the method is completely noninvasive, relying *inter alia* on intrinsic deoxyhemoglobin for image contrast rather than an exogenously administered contrast agent.

The presence of paramagnetic deoxyhemoglobin in blood vessels produces an additional relaxation rate term in the surrounding tissue that is linearly dependent on the blood volume fraction and the magnetic susceptibility difference between the surrounding tissue and in the blood vessels [27]. The total R_2* relaxation rate of tissue can be written as:

$$R_2^* = R_2 + R_2' + k_i \mathrm{bv}_i \mathrm{Hct}_i (1 - Y_i) \Delta\chi \qquad (1)$$

where R_2 and R_2' represent the irreversible and reversible relaxation rates, respectively, in tumor tissue in the absence

Table 1. Summary of the Data Acquired from Study 1.

	Pretreatment	35 min Postsaline	Pretreatment	35 min Post 30 mg/kg ZD6126	Pretreatment	35 min Post 50 mg/kg ZD6126
R_2* (sec^{-1})	110 ± 6	108.7 ± 6	90.8 ± 4	114.4 ± 7	106.4 ± 6	123.2 ± 10†
mHPA (%)		13.6 ± 2		4.8 ± 1*		9.1 ± 1

Tumor R_2* was measured prior to and immediately following administration of either saline ($n = 6$), 30 mg/kg ZD6126 ($n = 3$), or 50 mg/kg ZD6126 ($n = 7$), i.v., for up to 35 minutes.
Tumor perfusion was assessed by Hoechst 33342 uptake (mHPA).
Treatment with ZD6126 resulted in an increase in tumor R_2* over 35 minutes of challenge and was consistent with a decrease in tumor perfusion.
Values are mean ± 1 SEM.
*$P < .05$.
$^{\dagger}P < .01$.

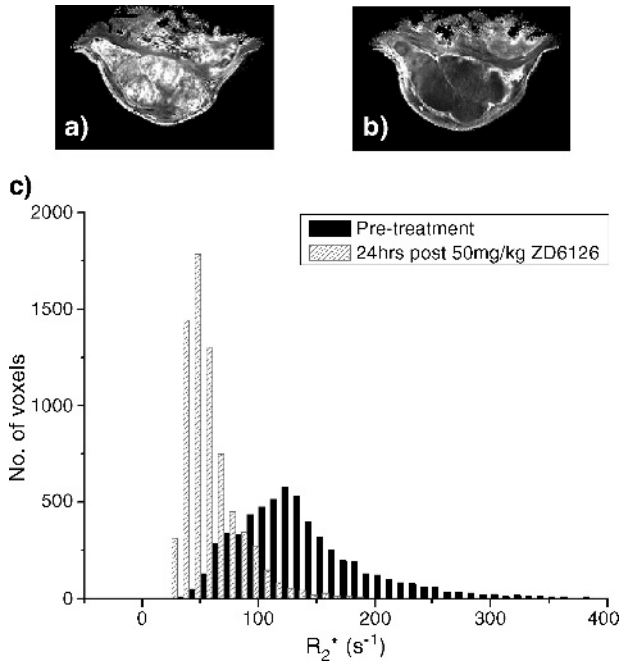

Figure 4. *Tumor R_2^* maps acquired from one rat GH3 prolactinoma (a) prior to and (b) 24 hours posttreatment with ZD6126, 50 mg/kg, i.v. The associated frequency histograms for these maps are shown in (c). Note the dramatic decrease in both the distribution and pixel values of R_2^* 24 hours after treatment with ZD6126.*

of deoxyhemoglobin, and the last term represents the relaxation in the tumor tissue due to the presence of deoxyhemoglobin. Hct is the hematocrit, Y is the fraction of oxygenated blood, bv is the fraction of tissue occupied by blood vessels, $\Delta\chi$ is the absolute susceptibility difference between fully oxygenated and deoxygenated blood, and k is a term dependent on blood vessel morphology and magnetic field strength. The subscript i indicates that there should be a summation over arterial, capillary, and venular vascular networks [28]. We can use Eq. (1) throughout the discussion to help interpret how the observed changes in tumor R_2^* following administration of ZD6126 relate to the underlying physical processes.

Study 1

Our underlying hypothesis was that following treatment with ZD6126, hemoglobin within erythrocytes would deoxygenate, resulting in an increase in tumor R_2^*. Tumor R_2^* increased over the first 35 minutes of challenge with either 30 or 50 mg/kg ZD6126 and was associated with a decrease in tumor perfusion as indicated by the reduced uptake of Hoechst 33342. This early R_2^* response is consistent with the induction of an ischemic insult induced by vascular shutdown/collapse, in agreement with our original hypothesis. An increase in tumor R_2^* could be observed as early as 7 minutes after administration of ZD6126. Increases in tumor R_2^* were also seen with the more clinically relevant dose of 30 mg/kg ZD6126. A similarly acute response to the vascular-targeting agent combretastatin A-4 phosphate has been shown by intravital microscopy of rat P22 carcinosarcomas grown in window chambers [29]. A hyperacute increase in tumor R_2^* in response to photodynamic therapy has also been recently reported [30].

The hyperacute increase in R_2^* following administration of ZD6126 is most likely due to tumor blood becoming more deoxygenated (a decrease in Y) as a consequence of reduced tumor blood flow due to the onset of vascular collapse or thrombosis. According to the Poiseuille equation for viscous laminar flow through a vessel, if blood pressure is maintained constant, a 10% reduction in vessel radius (which is a 20% reduction in vascular volume) will produce a 40% reduction in blood flow. Thus, although according to Eq. (1) a reduction in bv may be expected to decrease R_2^*, it is not unreasonable to expect changes in Y to initially predominate. Also, if the erythrocytes are trapped within the blood vessels so that it is just a reduction in plasma that occurs and not a reduction in erythrocyte density, then the product Hct·bv remains constant and changes in R_2^* are again dominated by the reduction in Y. Alternatively, occlusion of just a few arteriolar supply vessels could cause widespread reduction of blood flow in the capillary bed and hence a large decrease in Y.

Analysis of the R_2^* maps from study 1 showed that those voxels exhibiting a relatively fast basal R_2^* subsequently

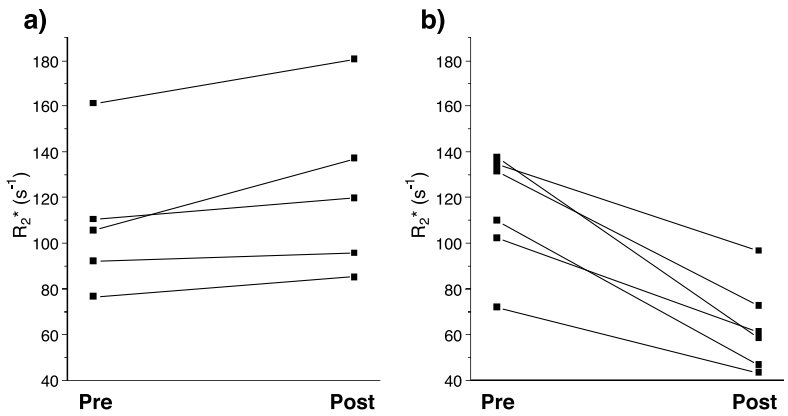

Figure 5. *Line series of R_2^* for each individual rat in study 2. Tumor R_2^* was measured from a single transverse slice prior to and 24 hours after intravenous administration of either (a) saline (n = 5) or (b) 50 mg/kg ZD6126 (n = 6).*

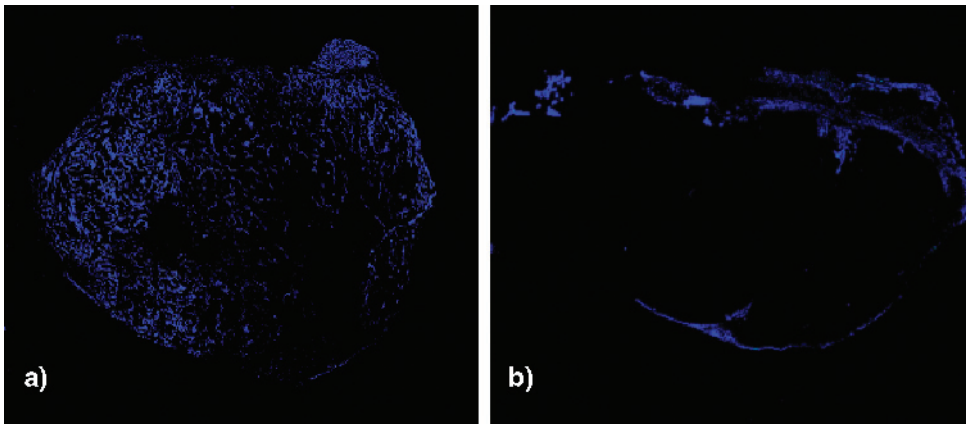

Figure 6. *Composite fluorescence images of Hoechst 33342 uptake into rat GH3 prolactinomas 24 hours after administration of either (a) saline or (b) 50 mg/kg ZD6126. The composite image shown in (b) is taken from the same tumor shown in Figure 4.*

showed the greatest initial increase in R_2* in response to ZD6126. Furthermore, a strong positive correlation between the baseline tumor R_2* and the subsequent hyperacute increase in R_2* measured 35 minutes after treatment with 50 mg/kg ZD6126 was obtained (Figure 7). This suggests that the baseline R_2* has: 1) prognostic value for subsequent tumor response to ZD6126, and 2) is a predictor of the magnitude of the acute R_2* increase following treatment. We have previously shown that intense regions (relatively fast R_2*) in the baseline R_2* maps of GH3 prolactinomas are consistent with the presence of perfused vascularized tissue with relatively high deoxyhemoglobin concentrations (i.e., large blood volume), whereas dark regions (relatively slow R_2*) may indicate more poorly vascularized tissue in which the capillaries have a limited ability to transport erythrocytes [31]. Furthermore, we have demonstrated that the relatively fast tumor R_2* measured in rat GH3 prolactinomas is prognostic for an acute radiotherapeutic response [32]. Thus, the early R_2* response to ZD6126 most likely reflects well-perfused tumor regions to which the vascular-targeting agent is rapidly delivered. It could also be speculated that these same tumor regions are also under hypoxic stress, which induces neovascularization, but we have no direct hypoxia measurement (e.g., pimonidazole adduct formation) for the tumors in this study. Nevertheless, we have recently shown that mutant C6 gliomas with a relatively fast basal R_2* and larger blood volume compared to wild type were also more hypoxic [33], whereas a preliminary clinical study has shown that human prostate tumors exhibiting a relatively fast R_2* stained positive for pimonidazole whereas those tumors with slow R_2* stained negative [34].

Study 2

A small nonsignificant increase in tumor R_2* was found 24 hours after treatment with saline, consistent with an increase in deoxyhemoglobin as the tumor grows. In contrast to our hypothesis, tumor R_2* significantly decreased 24 hours posttreatment with 50 mg/kg ZD6126, but which also correlated with a significant decrease in tumor perfusion measured by Hoechst 33342 uptake. The magnitude of the decrease in R_2* of GH3 prolactinomas following treatment is similar to our previous observations and associated with massive central necrosis at this time point [14]. The disruption of the tumor blood vessel cytoskeleton by ZD6126 causes complete vessel collapse and stacking of the fully deoxygenated erythrocytes into rouleaux. The erythrocytes would now be expected to be fully deoxygenated so that $Y = 0$ in Eq. (1) and hence any changes in R_2* must relate to changes in the other parameters. If some tumor blood flow remains, it is possible that there is a reduction in Hct as the vessels collapse, and as Hct decreases with vessel size [35], R_2* would decrease.

From Eq. (1), there are several possibilities that would allow R_2* to decrease. For example, either the number of erythrocytes per unit volume of tumor tissue is not constant and decreases, or $R_2 + R_2'$ decreases. The first case could be true if erythrocytes are being cleared by macrophages, but this seems unlikely 24 hours after treatment with ZD6126. Another explanation is that there is an increase in the water/macromolecule ratio due to the presence of edema, which would cause a decrease in R_2. Accordingly, we found a significant decrease in tumor R_2 measured 24 hours

Table 2. Summary of the Data Acquired in Study 2.

	Pretreatment	24 hr Postsaline	Pretreatment	24 hr Post 50 mg/kg ZD6126
R_2* (sec^{-1})	109.2 ± 14	123.6 ± 17	114.6 ± 10	63 ± 8†
R_2 (sec^{-1})	45.3 ± 3	46.3 ± 3	44.7 ± 3	34.9 ± 2*
R_2' (sec^{-1})	67 ± 11	75.7 ± 13	68.7 ± 7	23.9 ± 7†
mHPA (%)		17.4 ± 3		5.3 ± 1†

Tumor R_2* and R_2 were measured prior to and 24 hours after administration of either saline ($n = 5$) or 50 mg/kg ZD6126 ($n = 6$), i.v.
Tumor R_2' was determined from synthesized difference maps (R_2* − R_2).
Tumor perfusion was assessed by Hoechst 33342 uptake (mHPA).
A significant decrease in R_2*, R_2, and R_2' was measured 24 hours after treatment with ZD6126, associated with a significant decrease in tumor perfusion.
Values are mean ± 1 SEM.
*$P < .02$.
†$P < .001$.

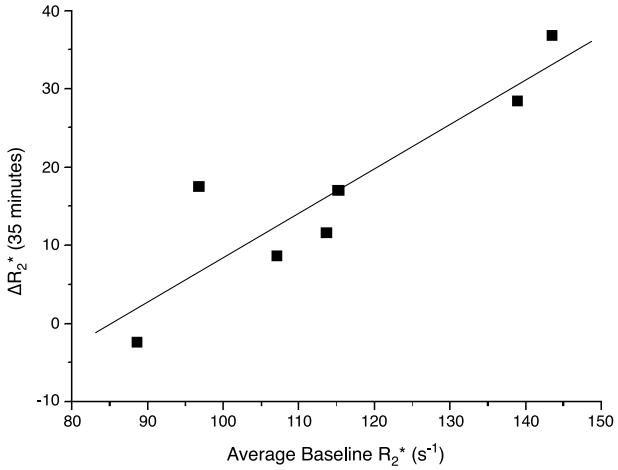

Figure 7. *Scatter graph of the average of the final and mean baseline R_2* plotted against the change in R_2* measured 35 minutes after challenge for each tumor. A significant and strong positive correlation was obtained ($r = 0.899$, $P < .01$).*

after 50 mg/kg ZD6126. However, this response constituted only ca. 20% of the decrease in tumor R_2*. Synthesis of R_2' maps (= $R_2^* - R_2$), which are highly sensitive to magnetic field inhomogeneities [36], revealed that the decrease in tumor R_2* was clearly dominated by a decrease in R_2' (Table 1). The striking reduction in R_2' clearly indicates the absence of any paramagnetic deposits at this time point and is associated with massive central necrosis in GH3 prolactinomas as previously reported [14,16]. The pathophysiological processes responsible for the decrease in tumor R_2' following treatment with ZD6126 are unclear, but may be a consequence of the denaturation of paramagnetic deoxyhemoglobin by methemoglobin to diamagnetic hemichromes, shown to cause a decrease in the transverse relaxation rate of chronic brain hemorrhage [37,38].

Conclusion

Measurement of tumor R_2* could be included in clinical trial protocols of vascular-targeting agents in which DCE MRI is already being used to assess drug activity [15]. The MGRE MRI method is available on most clinical scanners and measurements of human tumor R_2* have been reported [34,39]. Recent preliminary clinical data have shown similar time-dependent oscillations in human tumor R_2* following treatment with the vascular-targeting agent combretastatin A4 phosphate [40]. Clearly, the interpretation of R_2* changes is complex because, as we have shown, both increases and decreases in R_2* can occur at efficacious doses of vascular-targeting agents. Nevertheless, a change in tumor R_2* may provide a convenient and early MRI biomarker for detecting acute changes induced by vascular-targeting agents.

Acknowledgements

The authors would like to thank Glyn Fisher and his staff for care of the animals.

References

[1] Carmeliet P (2003). Angiogenesis in health and disease. *Nat Med* **9,** 653–660.
[2] Tozer GM, Kanthou C, Parkins CS, and Hill SA (2002). The biology of the combretastatins as tumour vascular targeting agents. *Int J Exp Pathol* **83,** 21–38.
[3] Denekamp J and Hobson B (1982). Endothelial-cell proliferation in experimental tumours. *Br J Cancer* **46,** 711–720.
[4] Carmeliet P and Jain RK (2000). Angiogenesis in cancer and other diseases. *Nature* **407,** 249–257.
[5] Dark GG, Hill SA, Prise VE, Tozer GM, Pettit GR, and Chaplin DJ (1997). Combretastatin A-4, an agent that displays potent and selective toxicity toward tumor vasculature. *Cancer Res* **57,** 1829–1834.
[6] Chaplin DJ and Dougherty GJ (1999). Tumour vasculature as a target for cancer therapy. *Br J Cancer* **80,** 57–64.
[7] Wachsberger P, Burd R, and Dicker AP (2003). Tumor response to ionizing radiation combined with antiangiogenesis or vascular targeting agents: exploring mechanisms of interaction. *Clin Cancer Res* **9,** 1957–1971.
[8] Siemann DW, Chaplin DJ, and Horsman MR (2004). Vascular-targeting therapies for treatment of malignant disease. *Cancer* **100,** 2491–2499.
[9] Goto H, Yano S, Zhang H, Matsumori Y, Ogawa H, Blakey DC, and Sone S (2002). Activity of a new vascular targeting agent, ZD6126, in pulmonary metastases by human lung adenocarcinoma in nude mice. *Cancer Res* **62,** 3711–3715.
[10] Siemann DW and Rojiani AM (2002). Enhancement of radiation therapy by the novel vascular targeting agent ZD6126. *Int J Radiat Oncol Biol Phys* **53,** 164–171.
[11] Blakey DC, Westwood FR, Walker M, Hughes GD, Davis PD, Ashton SE, and Ryan AJ (2002). Antitumor activity of the novel vascular targeting agent ZD6126 in a panel of tumor models. *Clin Cancer Res* **8,** 1974–1983.
[12] Davis PD, Dougherty GJ, Blakey DC, Galbraith SM, Tozer GM, Holder AL, Naylor MA, Nolan J, Stratford MR, Chaplin DJ, et al. (2002). ZD6126: a novel vascular-targeting agent that causes selective destruction of tumor vasculature. *Cancer Res* **62,** 7247–7253.
[13] Goertz DE, Yu JL, Kerbel RS, Burns PN, and Foster FS (2002). High-frequency Doppler ultrasound monitors the effects of antivascular therapy on tumor blood flow. *Cancer Res* **62,** 6371–6375.
[14] Robinson SP, McIntyre DJO, Checkley D, Tessier JJ, Howe FA, Griffiths JR, Ashton SE, Ryan AJ, Blakey DC, and Waterton JC (2003). Tumour dose response to the antivascular agent ZD6126 assessed by magnetic resonance imaging. *Br J Cancer* **88,** 1592–1597.
[15] Evelhoch JL, LoRusso PM, He Z, DelProposto Z, Polin L, Corbett TH, Langmuir P, Wheeler C, Stone A, Leadbetter J, et al. (2004). Magnetic resonance imaging measurements of the response of murine and human tumors to the vascular-targeting agent ZD6126. *Clin Cancer Res* **10,** 3650–3657.
[16] McIntyre DJ, Robinson SP, Howe FA, Griffiths JR, Ryan AJ, Blakey DC, Peers IS, Blakey DC, and Waterton JC (2004). Single dose of the antivascular agent, ZD6126 (*N*-acetylcolchinol-*O*-phosphate), reduces perfusion for at least 96 hours in the GH3 prolactinoma rat tumor model. *Neoplasia* **6,** 150–157.
[17] Horsman MR and Murata R (2003). Vascular targeting effects of ZD6126 in a C3H mouse mammary carcinoma and the enhancement of radiation response. *Int J Radiat Oncol Biol Phys* **57,** 1047–1055.
[18] Micheletti G, Poli M, Borsotti P, Martinelli M, Imberti B, Taraboletti G, and Giavazzi R (2003). Vascular-targeting activity of ZD6126, a novel tubulin-binding agent. *Cancer Res* **63,** 1534–1537.
[19] Gillies RJ, Bhujwalla ZM, Evelhoch JL, Garwood M, Neeman M, Robinson SP, Sotak CH, and Van Der Sanden B (2000). Applications of magnetic resonance in model systems: tumor biology and physiology. *Neoplasia* **2,** 139–151.
[20] Evelhoch JL, Gillies RJ, Karczmar GS, Koutcher JA, Maxwell RJ, Nalcioglu O, Raghunand N, Ronen SM, Ross BD, and Swartz HM (2000). Applications of magnetic resonance in model systems: cancer therapeutics. *Neoplasia* **2,** 152–165.
[21] Workman P, Twentyman P, Balkwill F, Balmain A, Chaplin DJ, Double J, Embleton J, Newell D, Raymond R, Stables J, et al. (1998). United Kingdom Co-ordinating Committee on Cancer Research (UKCCCR) guidelines for the welfare of animals in experimental neoplasia. *Br J Cancer* **77,** 1–10.
[22] Prysor-Jones RA and Jenkins JS (1981). Effect of bromocriptine on DNA synthesis, growth and hormone secretion of spontaneous pituitary tumours in the rat. *J Endocrinol* **88,** 463–469.
[23] Howe FA, Robinson SP, Rodrigues LM, and Griffiths JR (1999). Flow and oxygenation dependent (FLOOD) contrast MR imaging to monitor

the response of rat tumors to carbogen breathing. *Magn Reson Imaging* **17,** 1307–1318.

[24] Robinson SP, Rodrigues LM, Howe FA, Stubbs M, and Griffiths JR (2001). Effects of different levels of hypercapnic hyperoxia on tumour R_2* and arterial blood gases. *Magn Reson Imaging* **19,** 161–166.

[25] Kostourou V, Robinson SP, Whitley GS, and Griffiths JR (2003). Effects of overexpression of dimethylarginine dimethylaminohydrolase on tumor angiogenesis assessed by susceptibility magnetic resonance imaging. *Cancer Res* **63,** 4960–4966.

[26] Altman DG (1999). Practical Statistics for Medical Research. Chapman and Hall/CRC, London.

[27] Yablonskiy DA and Haacke EM (1994). Theory of NMR signal behavior in magnetically inhomogeneous tissues: the static dephasing regime. *Magn Reson Med* **32,** 749–763.

[28] Howe FA, Robinson SP, McIntyre DJ, Stubbs M, and Griffiths JR (2001). Issues in flow and oxygenation dependent contrast (FLOOD) imaging of tumours. *NMR Biomed* **14,** 497–506.

[29] Tozer GM, Prise VE, Wilson J, Cemazar M, Shan S, Dewhirst MW, Barber PR, Vojnovic B, and Chaplin DJ (2001). Mechanisms associated with tumor vascular shut-down induced by combretastatin A-4 phosphate: intravital microscopy and measurement of vascular permeability. *Cancer Res* **61,** 6413–6422.

[30] Gross S, Gilead A, Scherz A, Neeman M, and Salomon Y (2003). Monitoring photodynamic therapy of solid tumors online by BOLD-contrast MRI. *Nat Med* **9,** 1327–1331.

[31] Robinson SP, Rijken PF, Howe FA, McSheehy PM, van der Sanden BP, McSheehy PM, Heerschap A, Stubbs M, van der Kogel AJ, and Griffiths JR (2003). Tumor vascular architecture and function evaluated by non-invasive susceptibility MRI methods and immunohistochemistry. *J Magn Reson Imaging* **17,** 445–454.

[32] Rodrigues LM, Howe FA, Griffiths JR, and Robinson SP (2004). Tumor R_2* is a prognostic indicator of acute radiotherapeutic response in rodent tumors. *J Magn Reson Imaging* **19,** 482–488.

[33] Kostourou V, Troy H, Murray JF, Cullis ER, Whitley GSJ, Griffiths JR, and Robinson SP (2004). Overexpression of dimethylarginine dimethylaminohydrolase enhances tumor hypoxia: an insight into the relationship of hypoxia and angiogenesis *in vivo*. *Neoplasia* **6,** 401–411.

[34] Taylor NJ, Carnell DM, Smith RE, Hoskin PJ, Stirling JJ, D'Arcy JA, Leach MO, and Padhani AR (2003). Evaluation of prostate gland hypoxia with quantified BOLD MRI: initial results from a correlated histological study. *Proc Int Soc Magn Reson Med* **11,** 531.

[35] Jain RK (1988). Determinants of tumor blood flow: a review. *Cancer Res* **48,** 2641–2658.

[36] Punwani S, Ordidge RJ, Cooper CE, Amess P, and Clemence M (1998). MRI measurements of cerebral deoxyhaemoglobin concentration [dHb]—correlation with near infrared spectroscopy (NIRS). *NMR Biomed* **11,** 281–289.

[37] Bradley WG (1993). MR appearance of hemorrhage in the brain. *Radiology* **189,** 15–26.

[38] Yamada N, Imakita S, Nishimura T, Takamiya M, and Naito H (1992). Evaluation of the susceptibility effect on gradient echo phase images *in vivo*: a sequential study of intracerebral hematoma. *Magn Reson Imaging* **10,** 559–571.

[39] Rijpkema M, Kaanders JH, Joosten FB, van der Kogel AJ, and Heerschap A (2002). Effects of breathing a hyperoxic hypercapnic gas mixture on blood oxygenation and vascularity of head-and-neck tumors as measured by magnetic resonance imaging. *Int J Radiat Oncol Biol Phys* **53,** 1185–1191.

[40] Padhani AR (2003). MRI for evaluating antivascular cancer treatments. *Br J Radiol* **76,** S60–S80.